

# Fabrication of high efficient grating bandpass filters and their applications in soliton propagation system

L. Zhang, P. Harper, K. Sugden, J. A. R. Williams, F. M. Knox, P. N. Kean, I. Bennion and N. J. Doran

Department of Electronic Engineering & Applied Physics  
Aston University, Aston Triangle, Birmingham, B4 7ET, UK

## ABSTRACT

We report here fabrication of highly efficient in-fibre grating bandpass filters using the established UV-side-exposure technique. Various combinations of passband/stopband and transmission/rejection of single- and multi-channel filters have been produced in hydrogenated standard telecom, high Ge-doped and B/Ge-codoped fibres. Up to >60dB rejection stopbands ranging from ~2nm to 55nm, and passbands with 0.02nm-3nm linewidths and transmissivity up to >90% have been achieved with these devices. By concatenating several structures, a bandpass filter has been demonstrated with a combination of a 0.16nm passband centred in a ~35nm stopband, representing the highest reported finesse of 220 for any multi-nanometer stopband filter.

We also report the first application of a grating bandpass filter for suppressing timing jitter in soliton propagation system, enabling transmission of 10ps solitons over a distance of 2700km.

**Keywords:** Fibre Bragg grating, Bandpass filter, Light transmission and rejection, Soliton, Optical communication, time jitter suppression.

## 1. INTRODUCTION

In-fibre bandpass filters are increasingly perceived as important devices for applications in optical communication and signal processing including wavelength division multiplexing/demultiplexing (WDM/D), frequency discrimination and for the rejection of spontaneous emission noise in fibre amplifiers. To date, several techniques employed for fabricating fibre transmission filters have been reported [1-11]. However, the efforts have been focused mainly on narrow stopband devices the usefulness of which is limited for the wide range of applications such as WDM systems demanding multi-channel passbands with >30dB rejection of several tens-nm stopbands. It is, therefore, essential to explore techniques (or a combination of several techniques) which will facilitate the realisation of arbitrary passband/stopband combinations.

We have carried out a systematic investigation of practical approaches utilising the established UV-side-exposure fibre Bragg grating technique[12], with chirp and resonant grating fabrication and UV post-processing to achieve a range of profiles for fibre bandpass filters[13-15]. Utilisation of the chirped grating structure has been a key factor in our experiments. Chirped fibre gratings have been successfully produced by using the of dissimilar wavefronts in an UV two-beam side-exposure holographic system[16]. Although, in principle, arbitrary chirp rates can be realised using this configuration, the combination of large chirp rate and high reflectivity is limited in practice by the obtainable UV-induced index change in fibre. However, this constraint is significantly reduced with the discovery of photosensitisation of fibre using H<sub>2</sub>-loading technique[17] allowing the UV induced refractive index change in fibre to be as high as  $10^{-2}$ . This development has led to the achievement of reflection bandwidth ranging from 0.5nm to 140nm and reflectivity up to >99.99% in the chirped gratings[16,18,19], which may be used in creating high finesse bandpass filters. In the investigations reported here, the conventional Moiré grating technique[20] and the more recently developed UV-post-processing method[2] were separately employed in chirped gratings to introduce passband(s), resulting in two different structures of fibre bandpass filter - resonant-grating and gap-type. The characteristics of these two types of bandpass filter and their first ever application in soliton propagation system are discussed in the following sections.

## **2. FABRICATION TECHNIQUES**

### **2.1 Resonant-type bandpass filters**

The Moiré approach to fibre grating transmission filter fabrication was first reported by Reid *et al* for applications to side-etched, surface-relief structures[20]. The passband in a Moiré grating is induced by superposition of two phase-shifted uniform-period gratings. This approach was later adopted by Legoubin for UV side-written grating fabrication producing 0.2nm passband centred on a 0.8nm stopband[11]. It is apparent that the sub-nm stopband originates from the singly wavelength response of the uniform-period grating structure. We have extended the Moiré concept to incorporate chirped grating structures - superimposition of two phase-shifted chirped gratings (figure 1) - to realise broad stopband transmission filters[13]. Figure 2 shows the transmission spectra of two wide-stopband chirped Moiré resonators produced by this technique. The first structure (fig. 2a) was fabricated in a hydrogenated high-germania fibre, centred around 1544nm, having a stopband of ~4.3nm and a transmission linewidth of 0.17nm; the finesse (ratio of stopband/passband) of the resonator was ~25. The passband transmitted >90% of the signal with <2% transmission in the stopband. The second structure (fig. 2b) was fabricated in B/Ge co-doped fibre: it had a 0.4nm transmission linewidth at a centre wavelength of 1559.5nm in a stopband of width 8.4nm, and transmittance >80%. We have also fabricated broadband multi-channel bandpass filters (Fabry-Perot structure). Figure 3 shows such a filter with six passbands evenly distributed in a 10nm stopband. The number of passbands realised and the free spectral range were determined by the combination of the stopband width of the two constituent chirped gratings and the phase shift between them.

To further increase the stopband width, the broadband chirped reflectors were concatenated with a chirped Moiré filter. This grating-concatenation technique was developed as an alternative to the direct increase in chirp rate. Such an increase is known to cause not only the broadening of the transmission linewidth but also the lowering of the reflectivity of the stopband. In addition, the excessive chirp rate can also result in substantial modal outcoupling loss[21] inside the reflection band, thereby reducing the reflection and transmission efficiency. Using grating concatenation, the large stopband derives from the combined reflection characteristics of the chirped gratings, each produce with a moderate chirp rate, while the passband retains its original characteristics of narrow transmission linewidth and high transmissivity. This unique configuration offers freedom in designing broad stopband filters and enhances the filter efficiency by minimising the modal outcoupling loss. Fig 4 illustrates one such combination incorporating the first Moiré structure described in figure 2 (b) and two additional chirped gratings each of ~8nm band width centred at 1552nm and 1568nm, respectively. The stopband width of the combination is >22nm corresponding to an effective finesse of ~48. This multi-grating approach leads to a compact all-fibre device and fabrication tolerances on the constituent structures are not stringent. The key to this is the use of the chirped resonator to separate the transmission band sufficiently from the edges of its stopband to relax the precision with which the additional grating reflection characteristics must be produced.

### **2.2 Gap-type bandpass filters**

The UV post-processing technique, which was first demonstrated by Canning and Sceats[2], involves using a focused UV beam exposure to raise the refractive index (and partially erase the grating) at a selected region in a uniform-period grating. This exposure produces a phase shift region inside the grating allowing resonant light to penetrate the reflection band of the original grating. A transmission linewidth as narrow as 100MHz has been reported for such a structure[2]. Despite the high finesse of this bandpass filter, the stopband width once again was limited to sub-nm. We have applied this technique to chirped grating structures to introduce one or more passband into broad stopbands[14,15]. The principle here contrasts with the method described in ref.[2] in that the exposure erases the part of the grating reflecting a specific wavelength band (or bands) directly, producing a gap (or gaps) in the reflection spectrum. Unlike the resonator approach, the passband wavelength depends on which part of the grating is re-exposed and does not critically depend on the refractive index change induced by the secondary exposure. The transmission linewidth is determined by the spot size of the post-exposing UV beam and the grating chirp gradient.

Figure 5 illustrates the concept of the UV post-fabrication exposure of chirped gratings for producing bandpass fibre filters. In this example an ~100% reflectivity chirped grating with 11.3nm bandwidth was fabricated in a hydrogenated B/Ge co-doped fibre. An UV beam was then focused on the approximate centre of the grating. A 0.19nm narrow passband with a peak transmissivity of ~70% was introduced by an exposure of 3 minutes duration. The finesse, here defined as the ratio of passband to stopband, achieved with this structure is 60.

A single passband filter with a ~50nm stopband has been fabricated directly using this technique. The chirped grating was designed specially to cover the entire fluorescence spectrum of Er fibre (from 1520nm to 1570nm). The reflection and transmission spectra are shown in figure 6. A passband was opened at 1546nm with a 1.2nm transmission linewidth. The maximum reflection efficiency of the stopband is ~ 90% and the transmissivity of the passband is ~60%. It is apparent that there are some oscillations in the stopband response of the device. These are caused by some residual overlap in the reflection spectra of the two halves of the gratings on either side of the gap. These oscillations are more pronounced for gratings with larger chirp and wider stopbands, and, therefore, are minimised if the stopband of the grating structure is not too wide.

In order to eliminate the oscillation effect and achieve near 100% reflection efficiency for widest stopband transmission filters, the grating-concatenation method [13,14] was also applied here. Figure 7 shows the transmission spectrum of an example. A ~11nm reflection bandwidth chirped grating was first fabricated in a hydrogenated B/Ge co-doped fibre. This was followed by an additional, fringeless UV exposure, introducing a passband with 70% transmissivity and 0.16nm linewidth as measured with a 1pm resolution tunable laser source. This bandpass filter was then concatenated with two additional chirped gratings the reflection profiles of which overlapped with that of the bandpass filter on its short and long wavelength sides as shown in the inset of figure 7. The stopband resulting from this structure is effectively broadened while the transmission linewidth remains narrow. The stopband for this sample is ~35nm achieving an effective finesse of 220. This is by far the highest finesse achieved for any multi-nanometer stopband filter to date.

Multi-passband filters have also been produced using this technique. Figure 8 shows the transmission spectrum of a bandpass filter with four channels evenly spaced inside a ~50nm stopband again covering the whole Er fibre fluorescence spectral region. The four channels were introduced by individual equal time-length (~2.5min) exposures of the four selected positions along the grating. In the experiment, this was accomplished by translating the grating (fibre) to four successive positions along the direction perpendicular to the UV beam.

### 2.3 Comparison of two techniques

Table 1 summarises the characteristics of both the resonant-grating and gap-type bandpass filters. In comparison, the UV post-fabrication exposure technique appears to have a number of advantages over the resonant-grating method. The unavoidable broadening of the transmission linewidth in the latter is three times as great as in the former. For example, a 0.17nm transmission linewidth was obtained for a 4.3nm stopband in the latter, but 11.3nm in the former. Within the limit of the UV spot size, the transmission linewidth can be freely tailored in the gap-type filter by altering the spot size of the UV beam. The precise central wavelength of the passband is relatively easier to achieve using the UV post-processing technique. In addition, the passband(s) can be positioned arbitrarily inside the stopband by exposure of selected part(s) of the grating to the focused UV beam. In the resonant-grating approach the number of passbands and the free spectral range are inherently fixed by the phase shift between the two interacting gratings. On balance, the UV post-processing approach promises greater profile flexibility, although the associated spectra tend to exhibit oscillatory behaviours, as discussed above.

Regarding the transmissivity of the passbands, the values achieved so far are higher using the resonant-grating method than the UV post-processing approach. As discussed in section 2.1, the inherent modal outcoupling loss occurring inside the reflection band of the broadly chirped gratings reduces the transmissivity of the passband(s) regardless of technique. But some factors are technique-related. The low and unequal reflectivities of the two superimposed gratings underlie the low transmissivity of the passband. With the UV post-processing method, the transmissivity of the passband is a function of several parameters including the UV spot

size, intensity and the exposure time, and the fibre photosensitivity. Further characterisation of the effect on transmission of these parameters is essential for optimising the performance of gap-type filters.

With direct writing methods, for the same stopband width the finesse (ratio of stopband/passband) obtained from the gap-type filter is three times higher than from the resonant-grating filter (e.g. 69/21 for a ~11nm stopband in table 1). Table 1 demonstrates the further substantial increase in the stopband width and the finesse that results from the grating-concatenation method as applied to the respective techniques. It should be stressed here that the broad stopband and high finesse achievable by the grating-concatenation method are indicative of the great flexibility the method offers in designing and fabricating high efficiency and arbitrary profile bandpass filters, such as those with single or multi passband(s) asymmetrically distributed within the stopband.

### **3. APPLICATION**

High bit rate soliton based telecommunication systems have the potential to increase the capacity of long haul fibre links. Repeated amplification along such a link, however, puts a serious constraint on capacity via the Gordon-Haus limit[22]. It has been shown[23] that by including a frequency transmission filter at each amplification stage it is possible to increase the bit rate and/or propagation at each amplification as the Gordon-Haus limit can be extended. A single-channel bandpass filter fabricated using the UV post-processing method was inserted into a single span recirculating loop in order to suppress the amplifier spontaneous emission noise and reduce the rate of Gordon-Haus jitter accumulation. The results were compared with theoretical calculations and with experimental results using a standard bulk device.

The bandpass filter used in this experiment had a single passband centred at 1554nm with a 3dB bandwidth of 1.8nm. The stopband was extended to cover the whole of the erbium fluorescence band. The device had a polarisation-dependent loss of 0.3dB and an insertion loss of 2dB. Figure 9 shows a schematic diagram of the recirculating loop. The soliton source was an actively mode-locked 1GHz fibre ring laser which gave near transform-limited 10ps pulses at the operating wavelength of 1554nm. Results were taken by propagating the pulses from the fibre laser in the recirculating loop until the required distance was reached. Jitter measurements were then made using a sampling oscilloscope. The spectrum of the pulses remained virtually unchanged as the propagation distance increased. The experimental results (figure 10) show that the fibre grating bandpass filter enabled a propagation distance of 2700km to be achieved, corresponding to 9.5ps r.m.s jitter. With no filter in the loop the signal would propagate no further than 250km before spontaneous emission noise from the amplifier rose catastrophically. Repeating the experiment using a standard air-gap Fabry-Perot passband bulk filter, with a 3dB bandwidth of 3nm, in place of the fibre grating filter gave the same 9.5ps r.m.s jitter after only 1700km. This bulk device had a relatively high polarisation-dependent loss of 1.5dB and an insertion loss of 2.2dB. Theoretical values of Gordon-Haus jitter were calculated for both filters up to a distance of 2500km giving a good approximation to the experimental results.

Due to the flexibility of the fabrication technique of fibre grating bandpass filters it should be possible to achieve a greater reduction in jitter with an optimised bandwidth filter. Furthermore, it should also be possible to progress to a sliding guiding filter system, with successive gratings having slightly different central frequencies, leading to still greater jitter reduction. Fibre gratings have been demonstrated in a WDM system in conjunction with bulk filters [24] using a fibre grating to give jitter reduction in the WDM channels but a bulk device to give suppression of the ASE. The results from our experiment indicate that it should be possible to realise such systems using only a fibre grating which could be made in a single fibre.

### **4. CONCLUSION**

In conclusion, effective and practical in-fibre bandpass filters have been successfully fabricated using established fibre grating technology incorporating the resonant-grating and UV post-processing methods. A single channel broad stopband filter produced by these techniques has effectively performed a suppression of the amplifier spontaneous emission noise and a reduction of time jitter in a soliton propagation system. The techniques explored here offer a practical approach to producing all-fibre bandpass filters with arbitrary passband/stopband combinations and high transmission/reflection efficiency for future applications.

## 5. ACKNOWLEDGMENTS

The authors gratefully acknowledge financial support from EPSRC and CASE studentship support for P. Harper from Alcatel Submarine Networks.

## 6. REFERENCES

1. I. Bennion, J. A. R. Williams, L. Zhang, K. Sugden and N. J. Doran, "UV-written in-fibre Bragg gratings," *Optical and Quantum Electronics*, **28**, pp. 93-135, 1996.
2. J. Canning and M. G. Sceats, " $\pi$ -phase-shifted periodic distributed structures in optical fibres by UV post-processing," *Electron. Lett.*, **30**, pp.1344-1345, 1994.
3. V. Mizrahi, T. Erdogan, D. J. Digiovanni, P. J. Lemaire, S. G. Kosinski, T. A. Strasse and A. E. White, "Fibre-grating transmission filters for use all-fibre demultiplexer," *Conf. Optical Fibre Communications 1994 (OFC'94)*, San Jose, Techn Digest p.52, February 1994.
4. R. Kashyap, P. F. McKee and D. Armes, "UV written reflection grating structures in photosensitive optical fibres using phase-shifted phase masks," *Electron. Lett.*, **30**, pp.1977-1978, 1994.
5. W. W. Morey, T. J. Bailey, W. H. Glenn and G. Meltz, "Fibre Fabry-Perot interferometer using side exposed fibre Bragg gratings," *Conf. Optical Fibre Communications 1992 (OFC'92)*, San Jose, Techn Digest, p 96, February 1992.
6. D. Uttamchandani and A. Othonos, "Phase shifted Bragg gratings formed in optical fibres by post-fabrication thermal processing", *Opt. Comm.*, **127**, pp. 200-204, 1996.
7. M. Romabnoli, S. Wabnitz., P. Franco, M. Midrio, F. Fontana and G. Town, "Tunable erbium-ytterbium fibre sliding frequency soliton laser," *J. Opt. Soc. Amer. B*, **12**, pp.72-86, 1995.
8. W.W. Moorey, "Tuneable narrow-line bandpass filter using fibre gratings," *Opt Fibre Conf., OFC'91*, San Diego, California, post deadline paper PD20-1, February, 1991.
9. F. Bilodeau, K. O. Hill, B. Malo, D. C. Johnson and J. Albert, "High-return loss narrowband all-fibre bandpass Bragg transmission filter," *IEEE photon Technol Lett*, **5**, pp.191-194, 1994.
10. G. Town, K. Sugden, J. A. R. Williams, S. Poole and I. Bennion, "wide-band Fabry-Perot filters in optical fibre," *IEEE Photonics Technol. Lett.*, **7**, p.78, 1995.
11. S. Legoubin, E. Fertein, M. Douay, P. Bernage, P. Niay, F. Bayon and T. Georg, "Formation of morie grating in core of germanosilicate fibre by transverse holographic double exposure method," *Electron. Lett.*, **27**, pp.1945-1946, 1992.
12. G. Meltz, W. W. Morey and W. H. Glenn, "Formation of Bragg gratings in optical fibres by a transverse holographic method," *Opt. Lett.*, **14**, pp.823-825, 1989.
13. L. Zhang, K. Sugden, I. Bennion and A. Molony, "Wide-stopband chirped fibre morie grating transmission filters," *Electron. Lett.*, **31**, pp.477-478, 1995.
14. L. Zhang, K. Sugden, J. A. R. Williams, I. Bennion, D. C. J. Reid and C. M. Ragdale, "Postfabrication exposure of gap-type bandpass filters in broadly chirped fibre gratings", *Opt. Lett.*, **20**, pp.1927-1929, 1995.
15. L. Zhang, K. Sugden, J. A. R. Williams, I. Bennion, "In-fibre reansmission filters with broad stopbands using chirped Bragg gratings," *Conf on Photosensitivity and Quadratic Nonlinearity in Glass Waveguides, (PQNGW'95)*, Techn Dig, 22, pp. 132-135, 1995.
16. M. C. Farries, K. Sugden, D. C. J. Reid, I. Bennion, A. Molony and M. J. Goodwin, "Very broad reflection bandwidth (44nm) chirped fibre gratings and narrow bandpass filters produced by the use of an amplitude mask," *Electron Lett*, **30**, pp. 891-892, 1994.
17. P. J. Lemaire, "Enhanced UV photosensitivity in fibres and waveguides by high-pressure hydrogen loading", *Conf on Optical Fibre Communication (OFC'95)*, San Diego, California, Tech Dig, WN5, pp.162-163, 1995.
18. K. Sugden, I. Bennion, A. Molony, M. C. Farries, D. C. J. Reid and M. J. Goodwin, "Fabrication and properties of chirped fibre gratings with reflection bandwidths exceeding 50nm and narrow bandpass fibre grating filters," *Technical Digest CLEO Europe'94, CWF57*, pp. 230-231, 1994.
19. K. Sugden, L. Zhang, J. A. R. Williams and I. Bennion, "Dissimilar wavefront technique for linear and quadratic chirps," *Conf on Photosensitivity and Quadratic Nonlinearity in Glass Waveguides, (PQNGW'95)*, Techn Dig, 22, pp.136-139, 1995.

20. D. C. J. Reid, C. M. Ragdale, I. Bennion, D. J. Robbins, J. Buus and W. J. Stewart, "Phase-shifted moiré grating fibre resonators," *Electron. Lett.*, **26**, pp.10-12, 1990.
21. V. Mizrahi and J. E. Sipe, "Optical properties of photosensitive fibre phase gratings," *J. Lightwave Technol.*, **LT-11**, pp.1513-1517, 1993.
22. J. P. Gordon and H. A. Haus. "Random walk of coherently amplified solitons in optical fibre transmission," *Opt. Lett.*, **11**, pp. 665-667, 1986.
23. A. Mecozzi, J. D. Moores, H. A. Haus and Y. Lai. "Soliton transmission control," *Opt. Lett.*, **16**, pp.1841-1843, 1991.
24. E. Kolltveit, B. Biotteau, I. Riant, F. Pitel, O. Audouin, P. Brindel, E. Brun, P. Sansonetti and J. -P. Hamaide. "Soliton frequency-guiding by UV-written fibre Fabry-Perot filter in a 2x5Gb/s wavelength-division multiplexing transmission over trans-oceanic distances," *Electron. Lett.*, **7**, pp.1498-1500, 1995.

**Table 1. Typical transmission and reflection characteristics of fibre bandpass filters**

		Gap-type					Resonant-type		
Method		UV post-processing					Phase-shift-grating superimposing		
Fibre		B/Ge (H <sub>2</sub> )			Ge (H <sub>2</sub> )	Stand. (H <sub>2</sub> )	Ge (H <sub>2</sub> )	B/Ge (H <sub>2</sub> )	
Directly writing	Stopband width (nm)	55	34	11	8.2	11	4.3	8.4	12
	Refl. of stopband	85%	95%	99%	99%	97%	98%	99%	99%
	Trans. of passband	57%	44%	60%	85%	56%	90%	80%	80%
	Transmission linewidth (nm)	1.2-3.5	0.9	0.16	0.38	0.26	0.17	0.42	0.8
	Finesse	45-15	38	69	22	42	25	21	15
Concatenating	Effe. Stopband width (nm)	11+12+13=36					8+8+8=24		
	Effe. finesse	220(36/0.16)					48(24/0.5)		

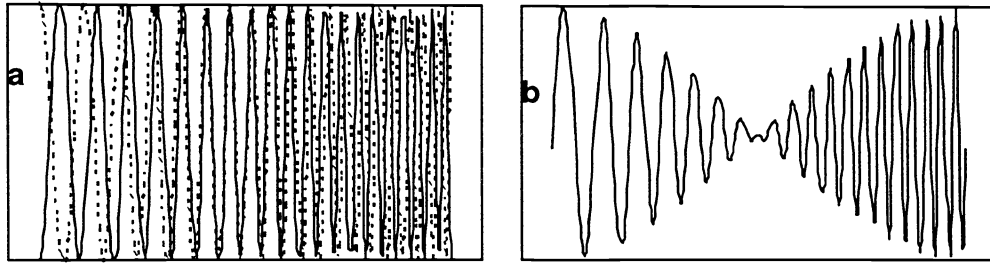


Figure 1. a) Two individual phase-shifted chirped structures; b) The final fringe structure resulting from the superimposition of two chirped gratings.

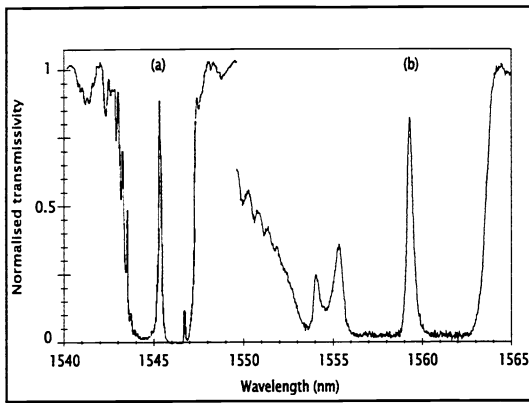


Figure 2. Transmission spectra of two broad stopband Moiré gratings

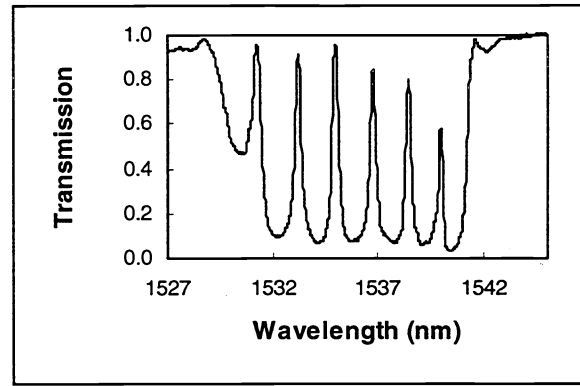


Figure 3. Transmission spectrum of a multi-channel resonant-grating bandpass filter.

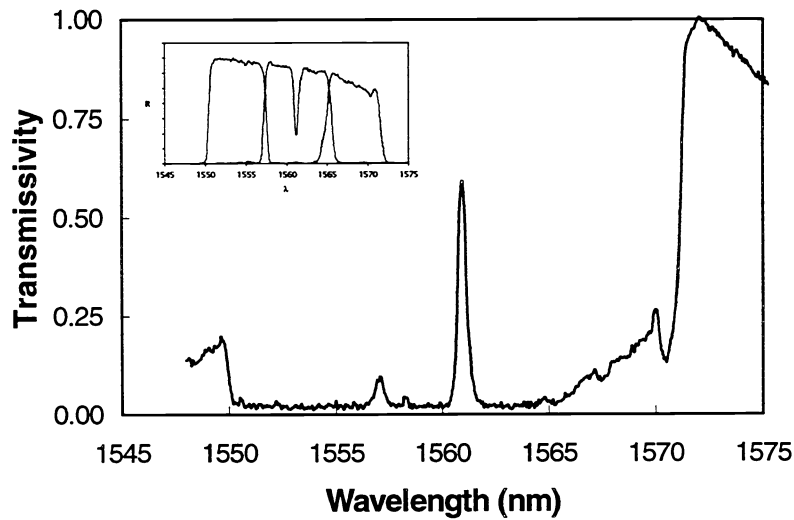


Figure 4. Transmission spectra of a concatenated broad stopband transmission filter. Inset: reflection spectra of the three concatenated chirped gratings

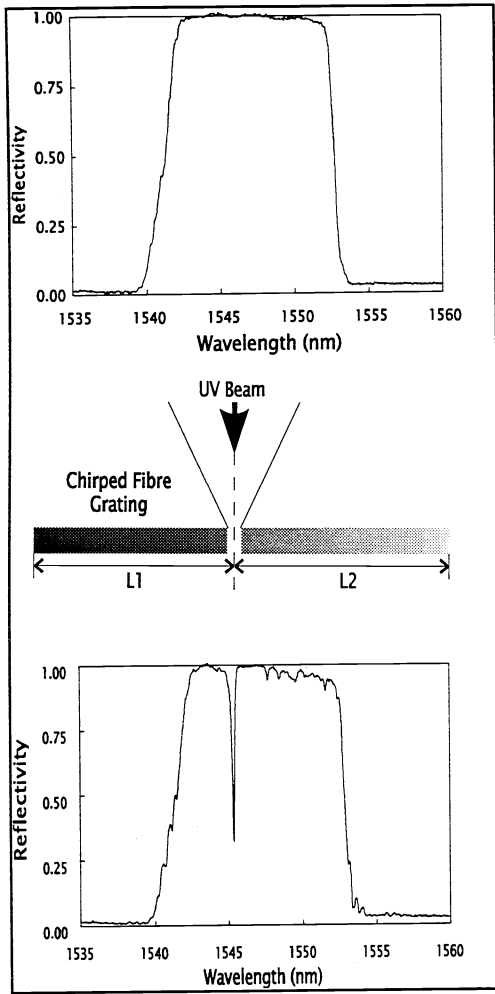


Figure 5. Fabrication concept of post-grating-fabrication UV exposure method.

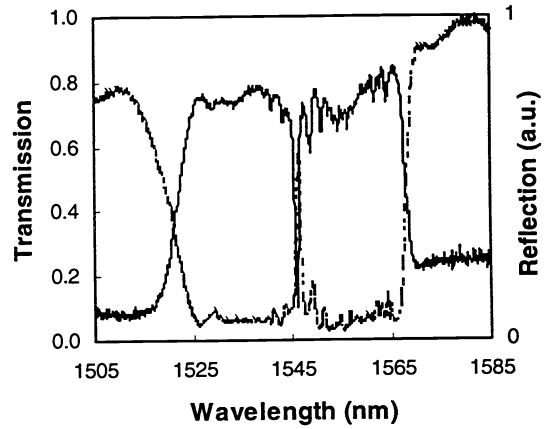


Figure 6. Reflection (solid) and transmission (dashed) spectra of a 1.2nm passband filter at 1546nm in a 50nm stopband broadly chirped fibre grating.

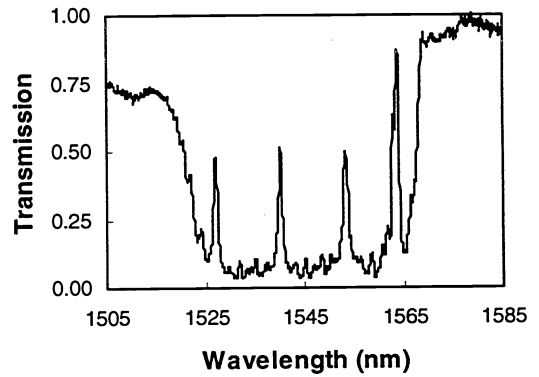


Figure 7. Four-channel multi-passband filter produced using UV post-processing method.

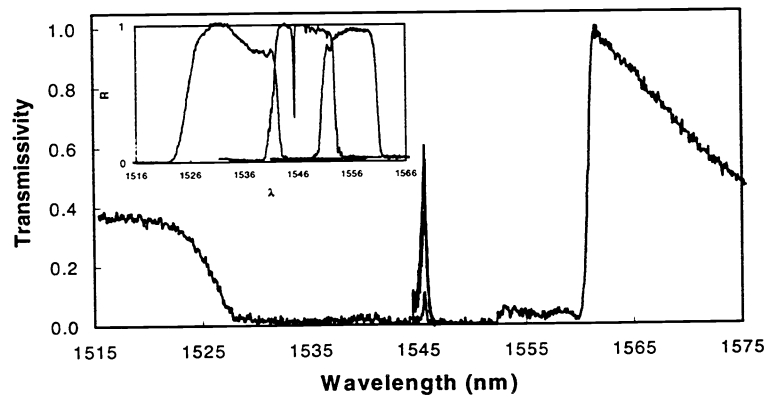


Figure 8. Transmission spectrum of a gap-type bandpass filter with a stopband of 36nm and a finesse of 220. Inset: Reflection profiles of the individual gratings.

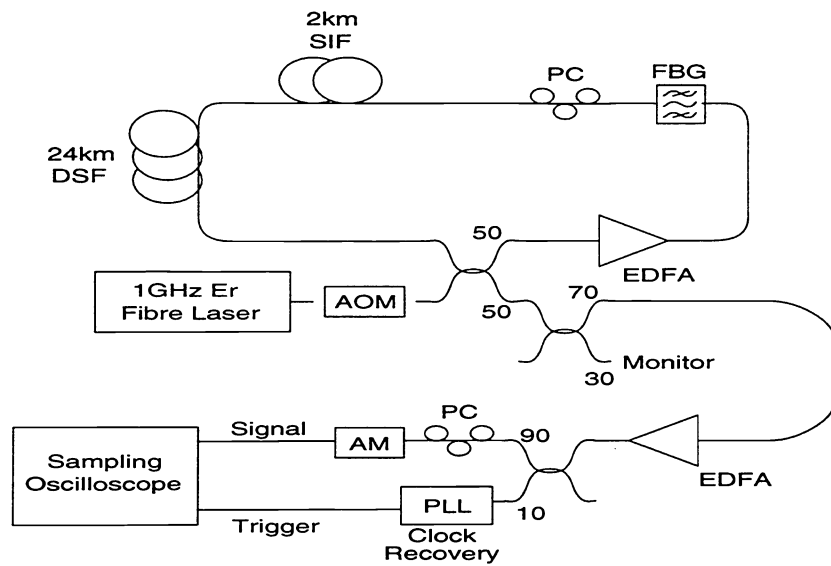


Figure 9. Schematic diagram of the soliton propagating system set-up. AOM: Acousto optic modulator, EDFA: Erbium doped fibre amplifier, BPF: Band pass filter, PC: Polarisation controller, SIF: Step-index fibre, DSF: Dispersion shifted fibre, PLL: Phase locked loop, AM: Lithium niobate amplitude modulator.

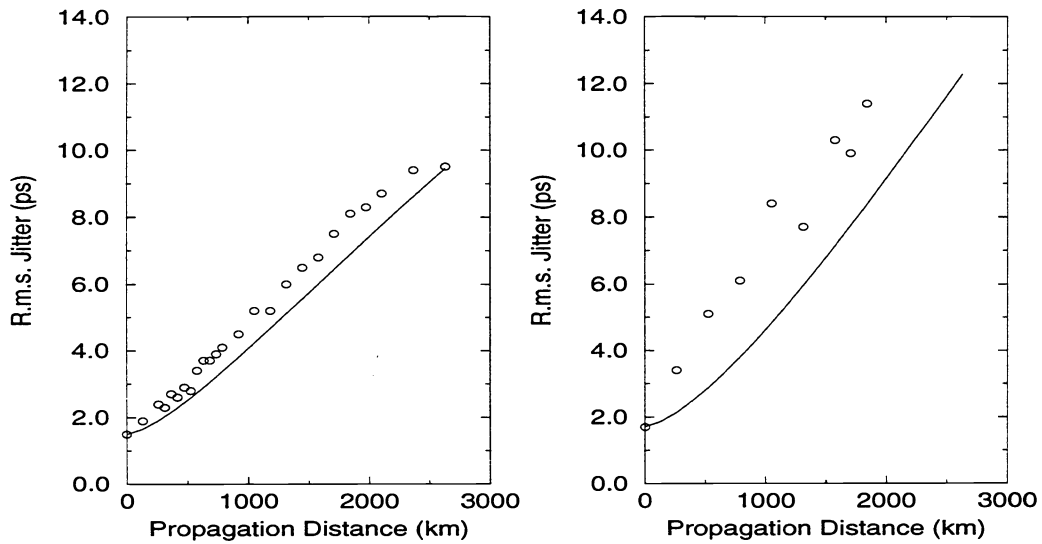


Figure 10. Experimental and theoretical results for the fibre Bragg grating bandpass filter (left) and bulk Fabry-Perot filter (right). The solid lines are the results of theoretical calculations and the circles are experimental results.